Understanding the Multi-wavelength Observation on the TeV halo of Geminga

Ruoyu Liu
Nanjing University
Deutsches Electronen-Synchrotron

Collaborators: Huirong Yan, Heshou Zhang, Shao-Qiang Xi, Chong Ge, Xiao-Na Sun, Xiang-Yu Wang

03.12.2019, 2019 TeVPA, Sydney

Outline

- ◆A Brief Introduction
  - 1)HAWC's Observation
  - 2)Previous Studies
- ◆X-ray Observation and its Implication
- ◆Anisotropic Diffusion Model
- ◆Summary

HAWC's observation on Geminga

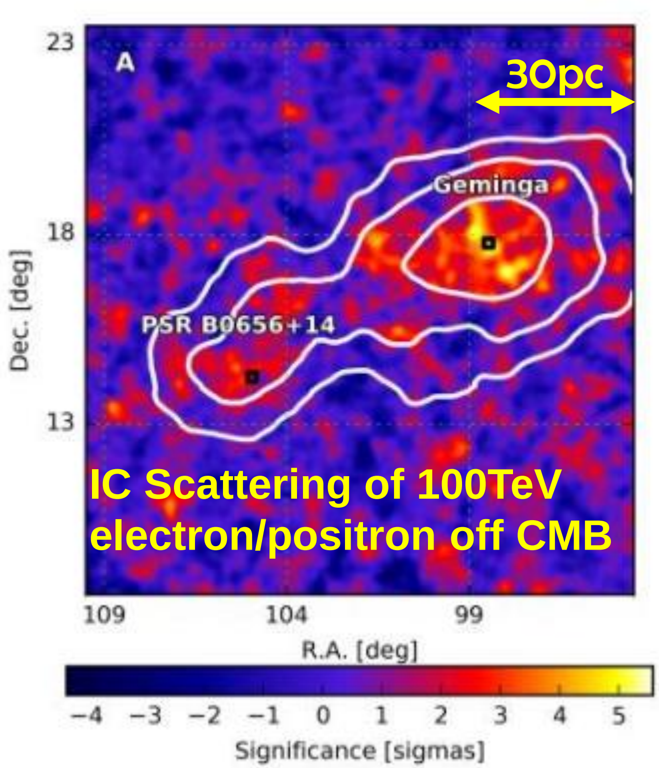

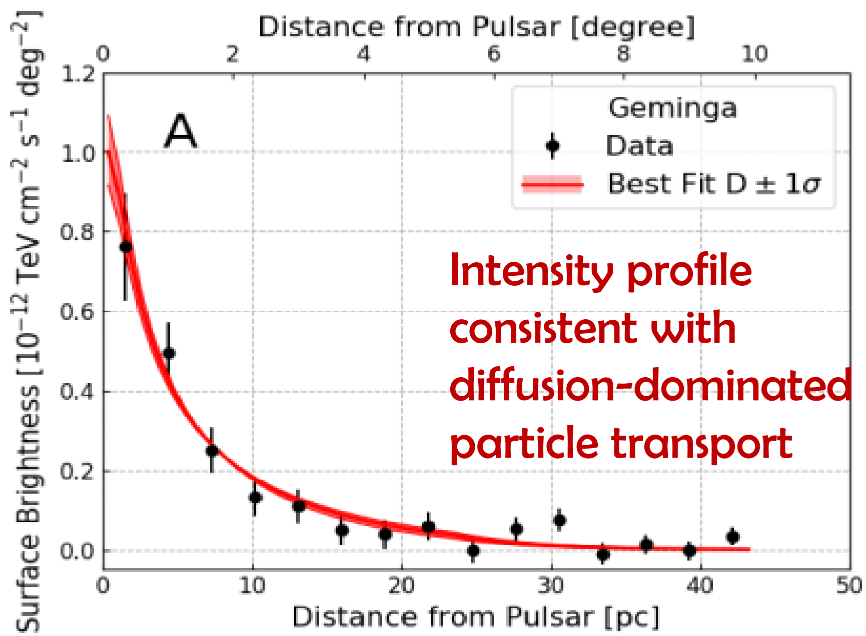

HAWC Collaboration 2017, Science, 2017, 358, 911

D_{100} (Diffusion coefficient of 100TeV electrons from joint fit of two PWNe)	[x10^{27} cm^2/sec]	4.5 ± 1.2

Two orders of magnitude smaller than the typical ISM diffusion coefficient

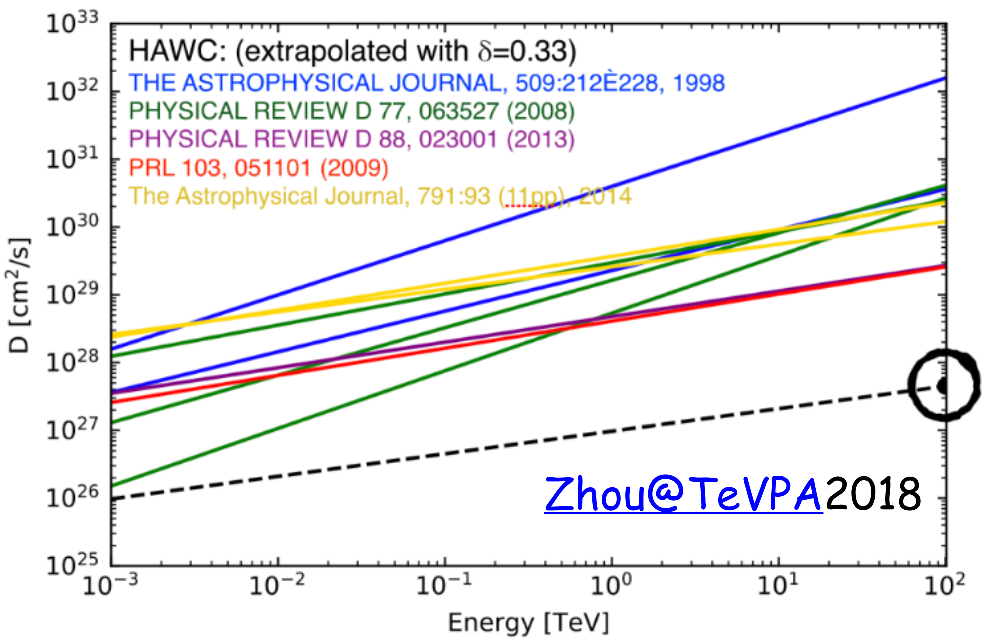

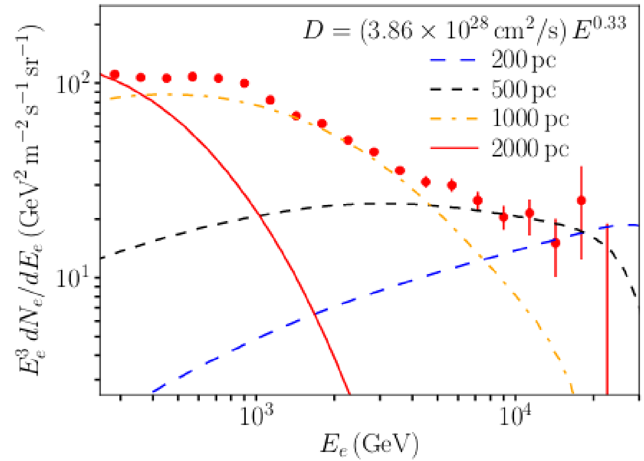

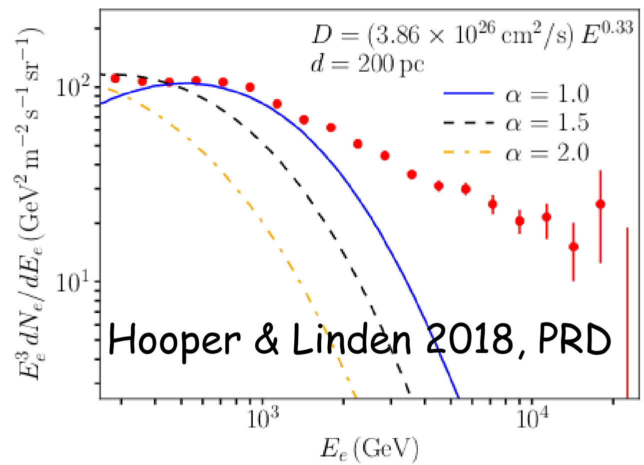

an inefficient diffusion zone embedded in normal diffusion zone in the ISM

$$D(E_e, r) = \begin{cases} D_1, & r < r_0 \\ D_2, & r \geq r_0. \end{cases}$$

e.g., Fang et al. 2018 ApJ, Profumo et al. 2018, PRD

Electron spectrum measurement disfavor a small diffusion coefficient

The generation of a very inefficient diffusion region

Small diffusion coefficient-> saturation of turbulence at small scale (r_g=0.04pc (E_e/100TeV)(B/3μG)$^{-1}$)

- CR self-generated waves:

CR density is not sufficiently high for an efficient self-regulation

the mechanism of self-generated Alfv́en waves due to the streaming instability **cannot** work to produce such a low diffusion coefficient even in the most optimistic scenario where the energy loss of electrons and the dissipation of the Alfv ́en waves are neglected. The reason is simple as **Geminga is too weak to generate enough high energy electrons at the late age**. (Fang et al., 2019, MNRAS)

- From background turbulence?

Need a strong ΔB Or small injection scale (~1pc & 3μG, Lopez-Coto & Giacinti 2018)?

Very chaotic topology: → X-ray emission

X-ray observation on the TeV halo

$$\epsilon_{\rm IC} \sim 20(E_e/100{\rm TeV})^2\,{\rm TeV}.$$
$$\epsilon_{\rm syn} \sim 0.6(E_e/100{\rm TeV})^2(B/3\mu{\rm G})\,{\rm keV}$$

$$F_{\rm keV}/F_{\rm 10TeV} \simeq B^2/8\pi U_{\rm CMB}$$

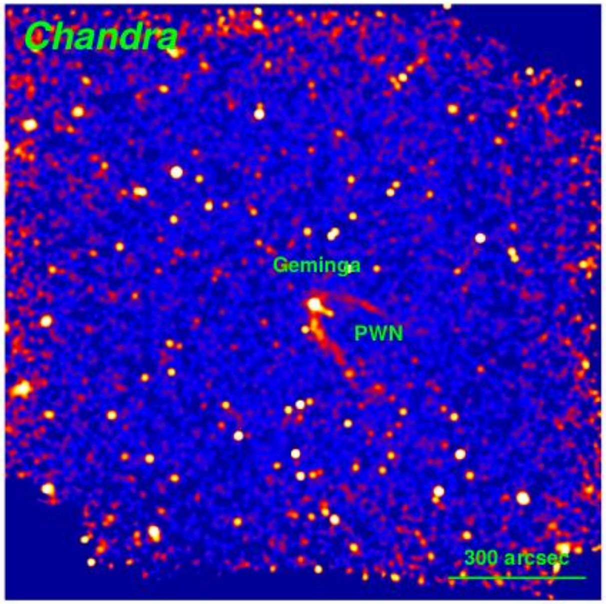

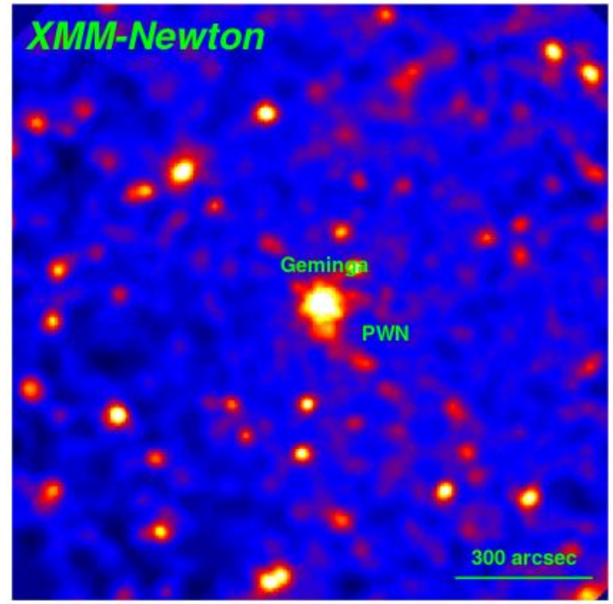

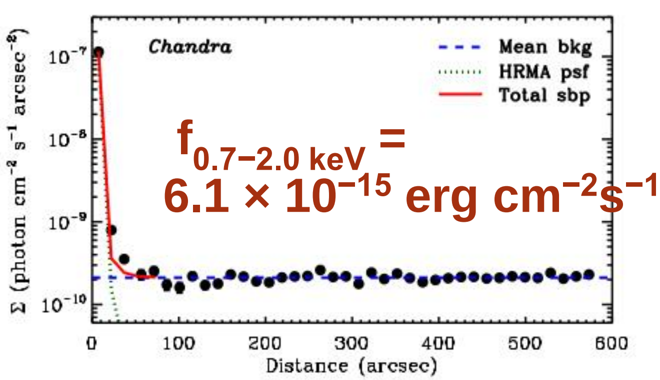

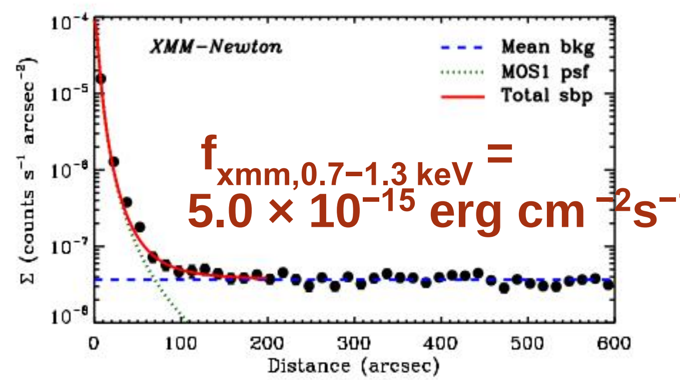

RYL et al. 2019, ApJ

Calculation of Intensity Profile

$$\frac{\partial N(E_e,r,t)}{\partial t} = \frac{1}{r^2}\frac{\partial}{\partial r}\left(r^2 D(E_e,r)\frac{\partial N}{\partial r}\right) - \frac{\partial}{\partial E_e}\left(\dot{E}_e N\right) + Q(E_e,t)\delta(r)$$

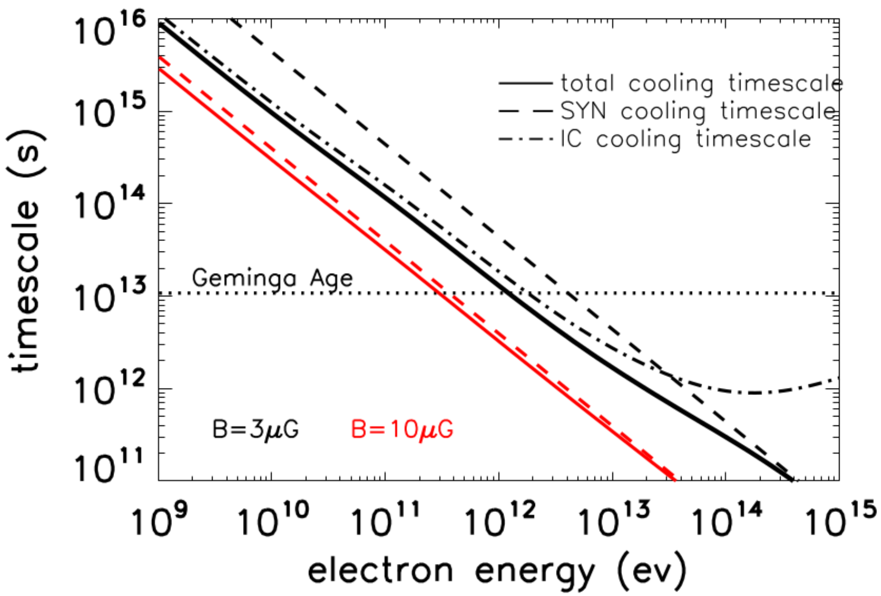

$$D = \begin{cases} D_1, & r \le r_0, \\ D_2, & r > r_0 \end{cases}$$

$$D = \begin{cases} D_1, & r < 20\text{pc} \\ D_1\left(\frac{D_2}{D_1}\right)^{(r-20)/30}, & 20\text{pc} \le r < 50\text{pc} \\ D_2 = D_{\rm ISM}, & r \ge 50\text{pc} \end{cases}$$

Line of sight integration

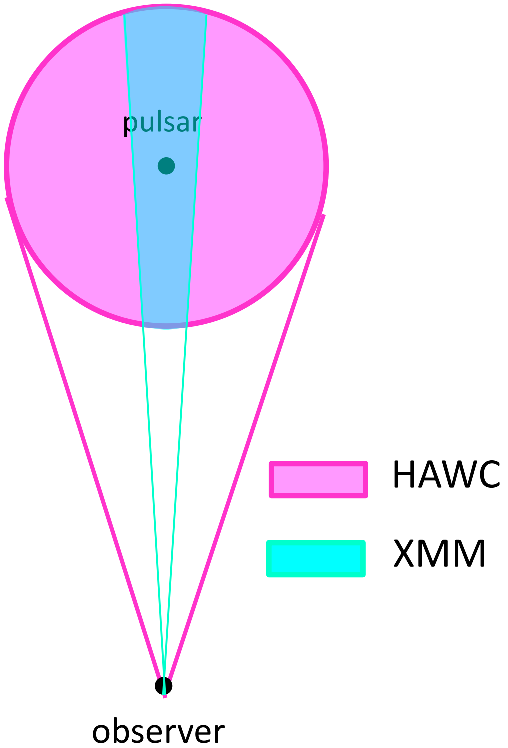

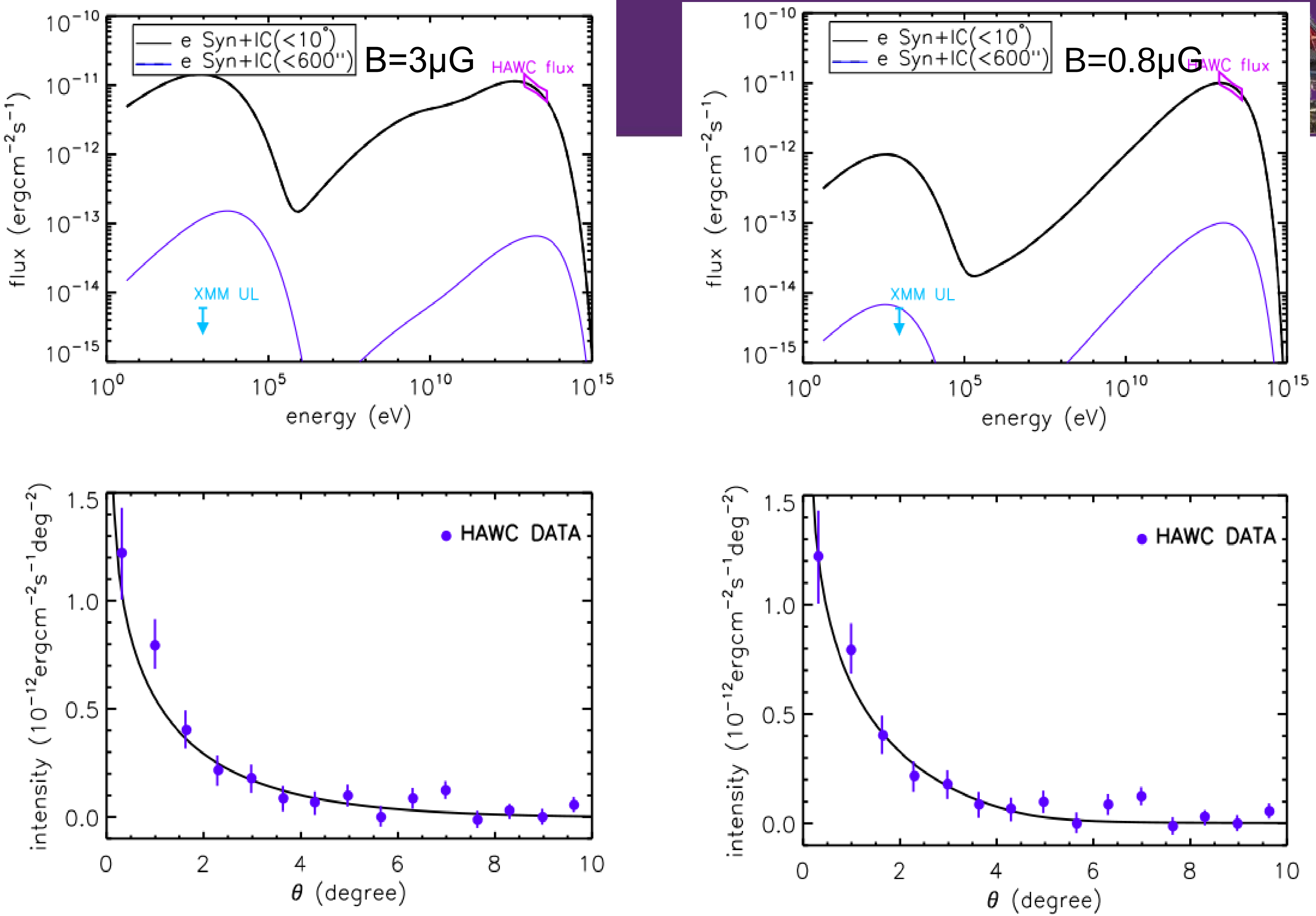

TeV Observation → **small diffusion coefficient → strong & chaoti field**

X-ray Observation → **weak B field**

Hadronic origin?

n_g~0.1cm^{-3}

$$\frac{1}{E_p}\frac{dE_p}{dt} \simeq 0.17\sigma_{pp}n_g c = 2\times10^{-17}\mathrm{s}^{-1}$$

Inefficient hadronic radiation

$$\sim 10^{52}(n_g/0.1\mathrm{cm}^{-3})^{-1}\mathrm{ergs}$$

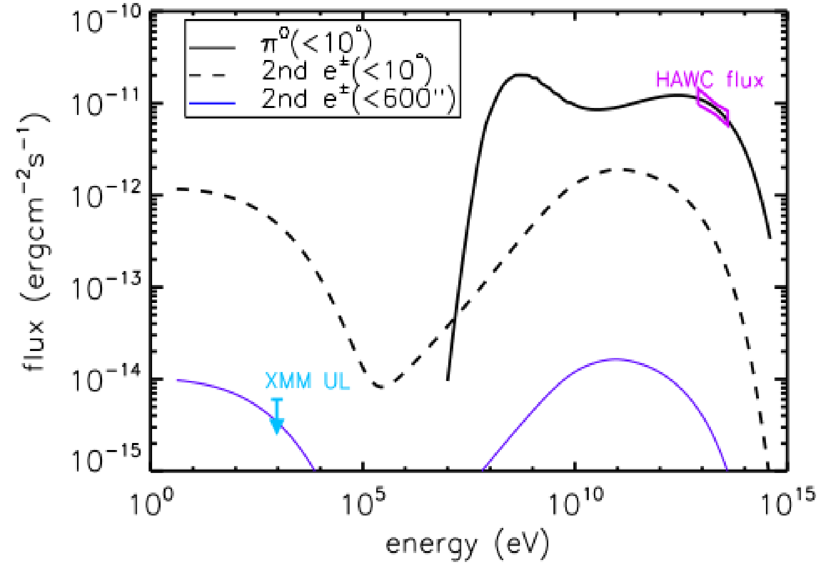

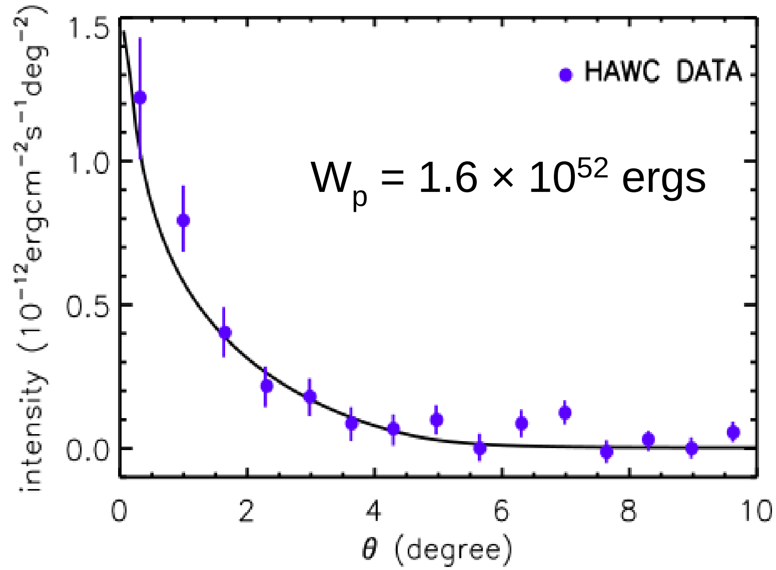

A more realistic scenario

ISM turbulence: coherent length 50-100pc, mean B field 3-6μG

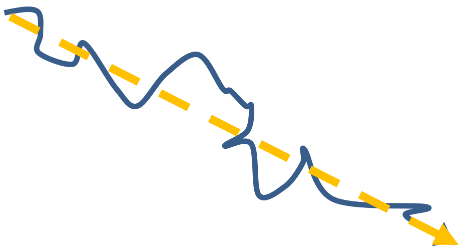

sub-Alfvenic ($M_A \sim \Delta B/B<1$) turbulence, **anisotropic**

$$D_{zz} = D_{\|} = D_0(E_e/1\mathrm{GeV})^q$$
$$D_{rr} = D_{\perp} = D_{zz} M_A^4$$

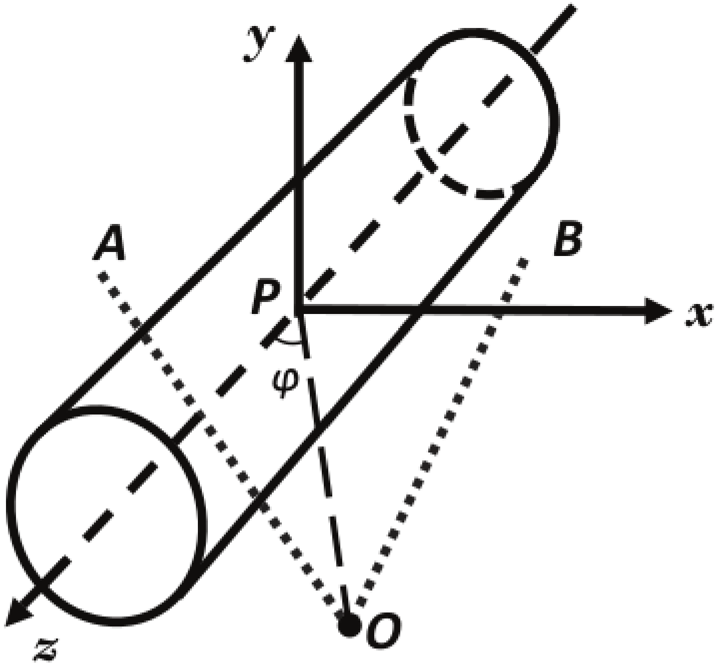

Diffusion coefficient -> Diffusion coefficient tensor

$$\frac{\partial N}{\partial t} = \nabla \cdot (\boldsymbol{\mathcal{D}} \cdot \nabla N) - \frac{\partial}{\partial E_e}\left(\dot{E}_e N\right) + Q$$

Synchrotron radiation also becomes anisotropic

$$P = \frac{2q^4 B^2 \gamma^2 \beta^2 \sin^2\alpha}{3m^2 c^3}$$

$$\omega_c = \frac{3\gamma^2 q B \sin\alpha}{2mc}$$

X-ray emission can be **reduced** significantly if the mean B field is roughly aligned with our line of sight

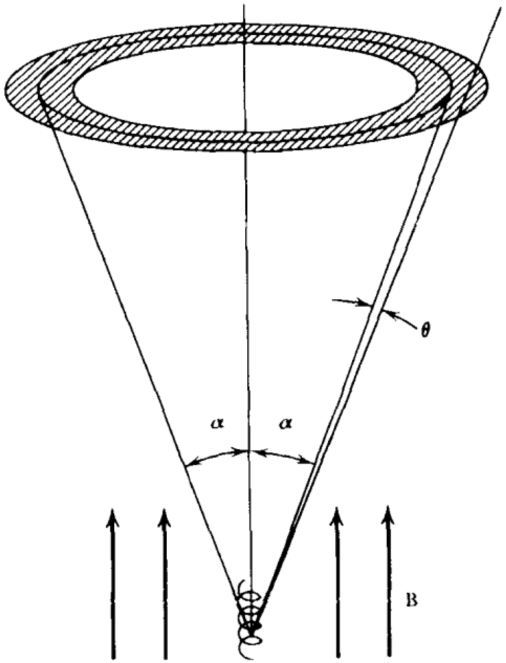

Rybicki & Lightman 1979

Horizontal: different viewing angle
Vertical: different Alfvenic Mach Number

$D_{//}=4\times10^{28}\ (E/1\mathrm{GeV})^{1/3}\mathrm{cm}^2/\mathrm{s}$

$B=3\mu G$

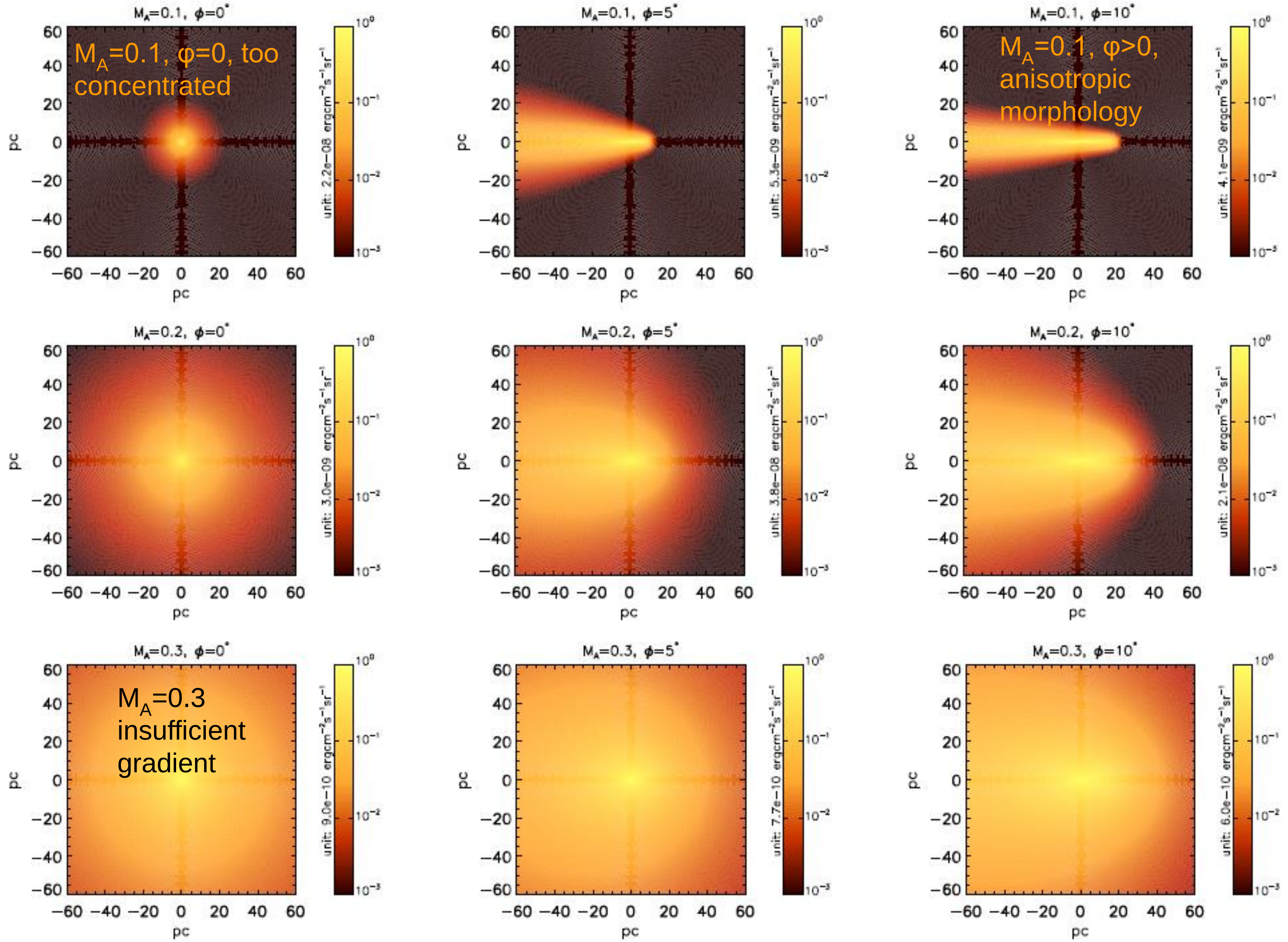

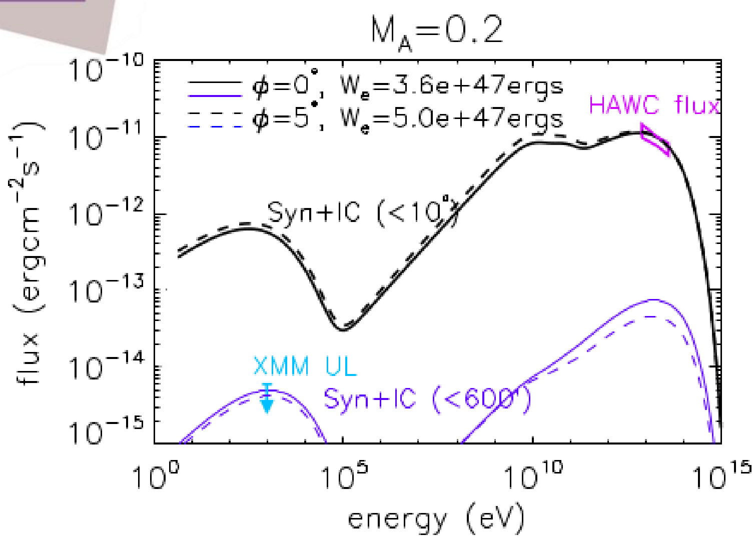

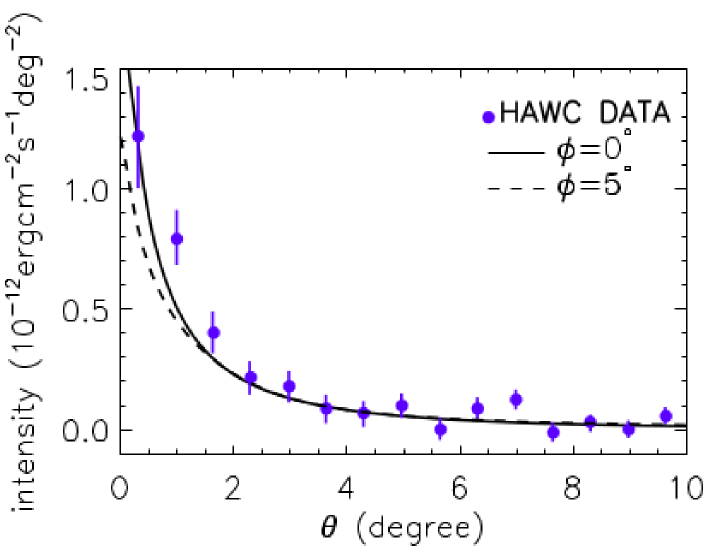

RYL et al. 2019, PRL

M_A~0.2, φ<5°

Sub-alfvenic turbulence
Mean B field well aligned with LOS

Mean B field in other TeV halos cannot be always aligned with LOS

A general picture for TeV halo

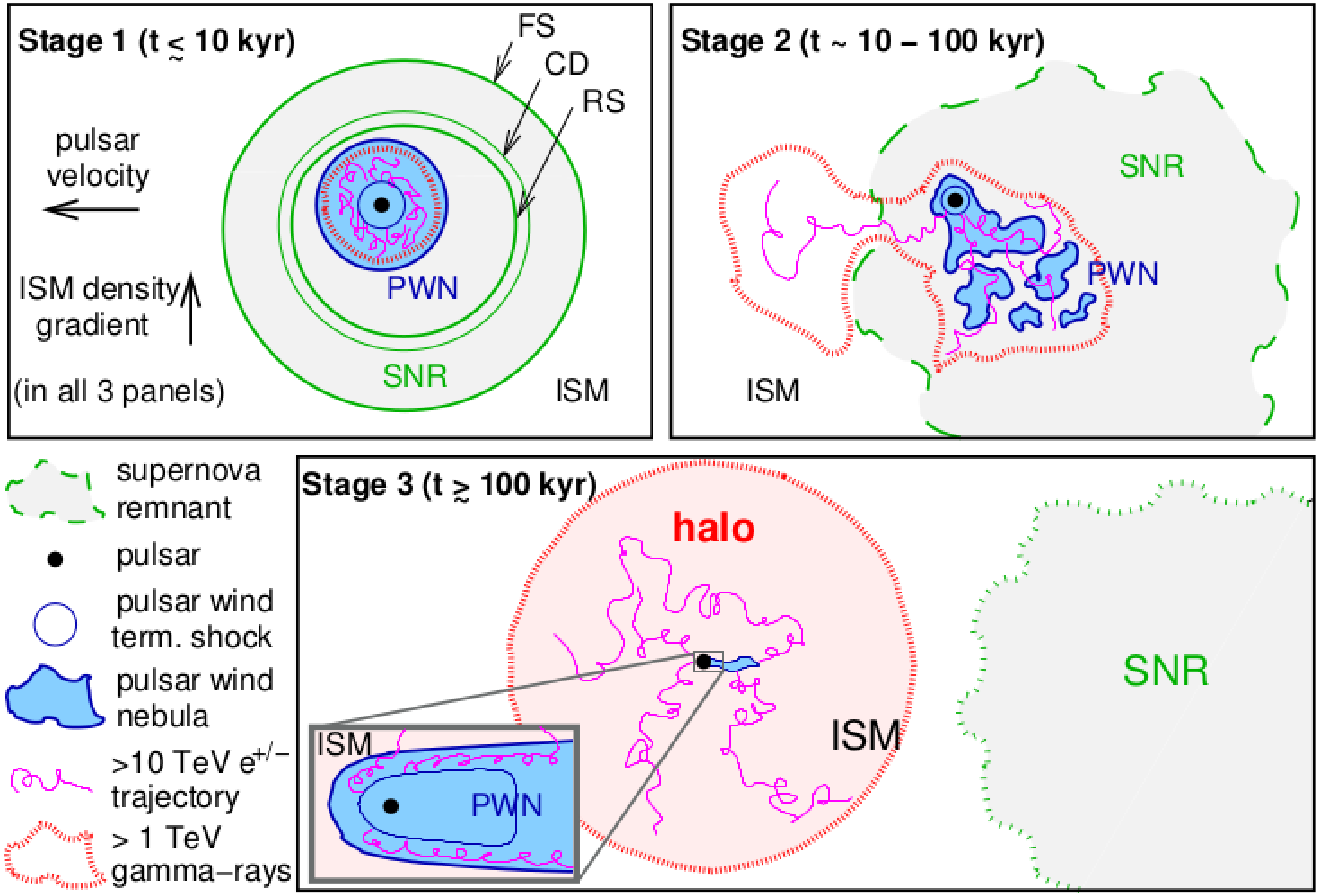

Giacinti et al. 2019

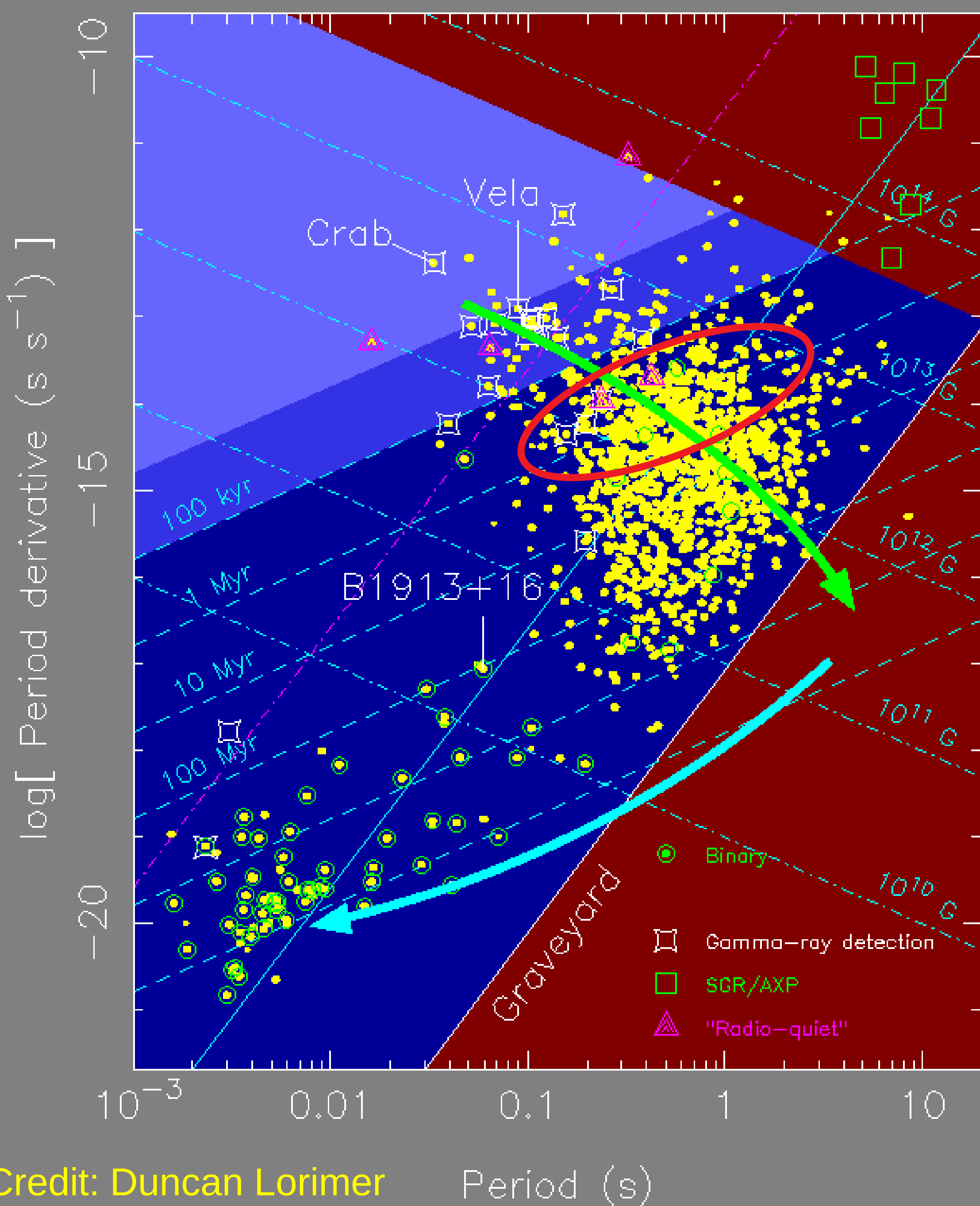

Credit: Duncan Lorimer

How many potential TeV halos in our Galaxy ?

Selection Criteria:

T_{age}>100kyr

$F=\eta_\gamma L_s/4\pi d^2>F_{lim}$

η_γ : Ratio of 100TeV luminosity to spindown luminosity

η_γ~0.07% (for Geminga)

300 pulsars with estimate flux above 5yr sensitivity of LHAASO

NANJING UNIVERSITY

Summary

- No significant diffuse X-ray emission around Geminga PWN has been detected by Chandra and XMM-Newton

- In the framework of isotropic diffusion, a highly turbulent region with very weak magnetic field is required.
  - hard to find physical interpretation
  - difficult to explain positron flux (unless with energy-independent diffusion coefficient)

- In the framework of anisotropic diffusion (more natural)
  - both diffuse X-ray and TeV emission can be explained with the typical ISM parameters
  - requirement: mean B field aligned with LOS

- Test the model with future observation of LHAASO and HAWC

Backup slides

ATNF Pulsar Catalogue

Catalogue Version: 1.61

#	NAME		PSRJ		DIST (kpc)	DIST_DM (kpc)		AGE (Yr)	EDOT (ergs/s)	C1
1	B1055-52	vl72	J1057-5226	vl72	0.09	0.09	ymw17	5.35e+05	3.0e+34	3.0964e-08
2	J0633+1746	hh92	J0633+1746	hh92	0.19	0.14	ymw17	3.42e+05	3.2e+34	7.4107e-09
3	B0906-49	dmd+88	J0908-4913	dmd+88	1.00	1.02	ymw17	1.12e+05	4.9e+35	4.0965e-09
4	B0656+14	mlt+78	J0659+1414	mlt+78	0.29	0.16	ymw17	1.11e+05	3.8e+34	3.7775e-09
5	B1951+32	kcb+88	J1952+3252	kcb+88	3.00	3.22	ymw17	1.07e+05	3.7e+36	3.4370e-09
6	J1732-3131	aaa+09c	J1732-3131	aaa+09c	0.64	0.64	ymw17	1.11e+05	1.5e+35	3.0616e-09
7	B1742-30	kac+73	J1745-3040	kac+73	0.20	2.34	ymw17	5.46e+05	8.5e+33	1.7766e-09
8	J1740+1000	mca00	J1740+1000	mca00	1.23	1.23	ymw17	1.14e+05	2.3e+35	1.2710e-09
9	J1913+1011	mhl+02	J1913+1011	mhl+02	4.61	4.61	ymw17	1.69e+05	2.9e+36	1.1408e-09
10	B1259-63	jlm+92	J1302-6350	jlm+92	2.63	2.21	ymw17	3.32e+05	8.3e+35	1.0032e-09
11	J1741-2054	aaa+09c	J1741-2054	aaa+09c	0.30	0.27	ymw17	3.86e+05	9.5e+33	8.8247e-10
12	J0954-5430	mlc+01	J0954-5430	mlc+01	0.43	0.43	ymw17	1.71e+05	1.6e+34	7.2344e-10
13	J2032+4127	aaa+09c	J2032+4127	aaa+09c	1.33	4.62	ymw17	2.01e+05	1.5e+35	7.0894e-10
14	J1831-0952	lfl+06	J1831-0952	lfl+06	3.68	3.68	ymw17	1.28e+05	1.1e+36	6.7907e-10
15	J1151-6108	ncb+15	J1151-6108	ncb+15	2.22	2.22	ymw17	1.57e+05	3.9e+35	6.6157e-10
16	B0114+58	stwd85	J0117+5914	stwd85	1.77	1.77	ymw17	2.75e+05	2.2e+35	5.8708e-10
17	B1822-09	dls72	J1825-0935	dls72	0.30	0.26	ymw17	2.33e+05	4.5e+33	4.1801e-10
18	B0355+54	mth72	J0358+5413	mth72	1.00	1.59	ymw17	5.64e+05	4.5e+34	3.7621e-10
19	J1509-5850	kbm+03	J1509-5850	kbm+03	3.37	3.37	ymw17	1.54e+05	5.1e+35	3.7543e-10
20	J1925+1720	lbh+15	J1925+1720	lbh+15	5.06	5.06	ymw17	1.15e+05	9.5e+35	3.1020e-10
21	B0740-28	fss73	J0742-2822	fss73	2.00	3.11	ymw17	1.57e+05	1.4e+35	2.9261e-10
22	J0855-4644	kbm+03	J0855-4644	kbm+03	5.64	5.64	ymw17	1.41e+05	1.1e+36	2.8910e-10
23	B0940-55	wvl69	J0942-5552	wvl69	0.30	0.41	ymw17	4.61e+05	3.1e+33	2.8796e-10
24	J1739-3023	mhl+02	J1739-3023	mhl+02	3.07	3.07	ymw17	1.59e+05	3.0e+35	2.6611e-10
25	J0538+2817	fcwa95	J0538+2817	fcwa95	1.30	0.95	ymw17	6.18e+05	4.9e+34	2.4240e-10

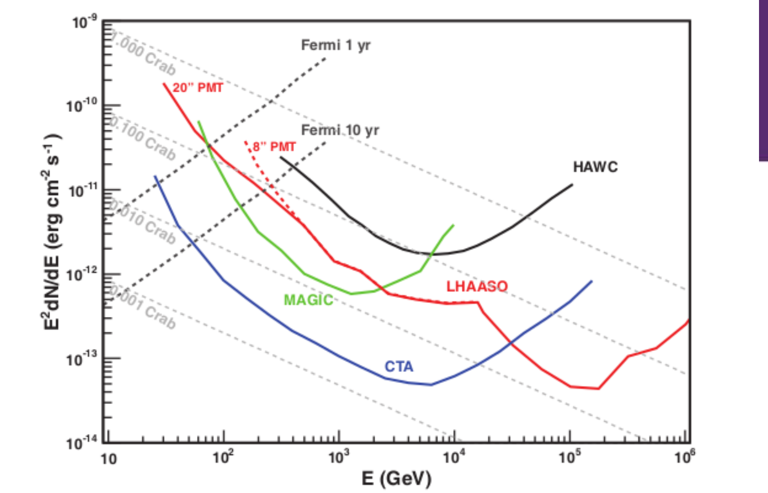

LHAASO 1-yr diff. flux sensitivity of point source @ 100TeV = 4e-14ergcm^{-2}s^{-1}

136	J1853-0004	hfs+04	J1853-0004	hfs+04	5.34	5.34	ymw17	2.88e+05	2.1e+35	6.1568e-11
137	J1701-3006E	cha03	J1701-3006E	cha03	7.05	4.76	ymw17	1.65e+08	3.6e+35	6.0554e-11
138	J1530-5327	mlc+01	J1530-5327	mlc+01	1.12	1.12	ymw17	9.44e+05	8.5e+33	5.6650e-11
139	J2017+0603	cgj+11	J2017+0603	cgj+11	1.40	1.40	ymw17	5.74e+09	1.3e+34	5.5451e-11
140	B0021-72F	mlr+91	J0024-7204F	mlr+91	4.69	2.54	ymw17	6.44e+08	1.4e+35	5.3211e-11

137 pulsars with “spindown flux > 5.7e-11 erg/cm^2/s (1yr sensitivity)

296	B0953-52	mlt+78	J0955-5304	mlt+78	0.40	0.40	ymw17	3.87e+06	2.2e+32	1.1495e-11
297	J1756-2225	hfs+04	J1756-2225	hfs+04	4.78	4.78	ymw17	1.22e+05	3.1e+34	1.1343e-11
298	J1544+4937	brr+13	J1544+4937	brr+13	2.99	2.99	ymw17	1.17e+10	1.2e+34	1.1222e-11
299	J1616-5017	ncb+15	J1616-5017	ncb+15	3.48	3.48	ymw17	1.67e+05	1.6e+34	1.1045e-11
300	B1143-60	mlt+78	J1146-6030	mlt+78	1.63	1.63	ymw17	2.42e+06	3.5e+33	1.1013e-11

300 pulsars with “spindown flux” > 1.1e-11 erg/cm^2/s (5yr sensitivity)

There are actually many more invisible pulsars in our Galaxy

Gamma-ray pulsar : 230+
Radio pulsar : 2600+

outer gap solid angle : 1 sr (gamma-ray)
Polar cap solid angle : 0.1 sr （radio）

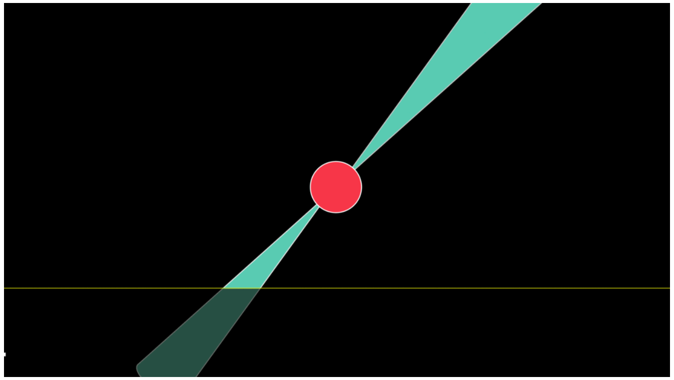

Credit: Jen Christiansen, Scientific American.

But emission of the TeV halo is not beamed!

total pulsar with detectable TeV halo:
10- 100 x observed number ~ 3000 - 30000

Gamma-ray flux + morphology + X-ray/radio flux

=> study mean B field direction and M_A

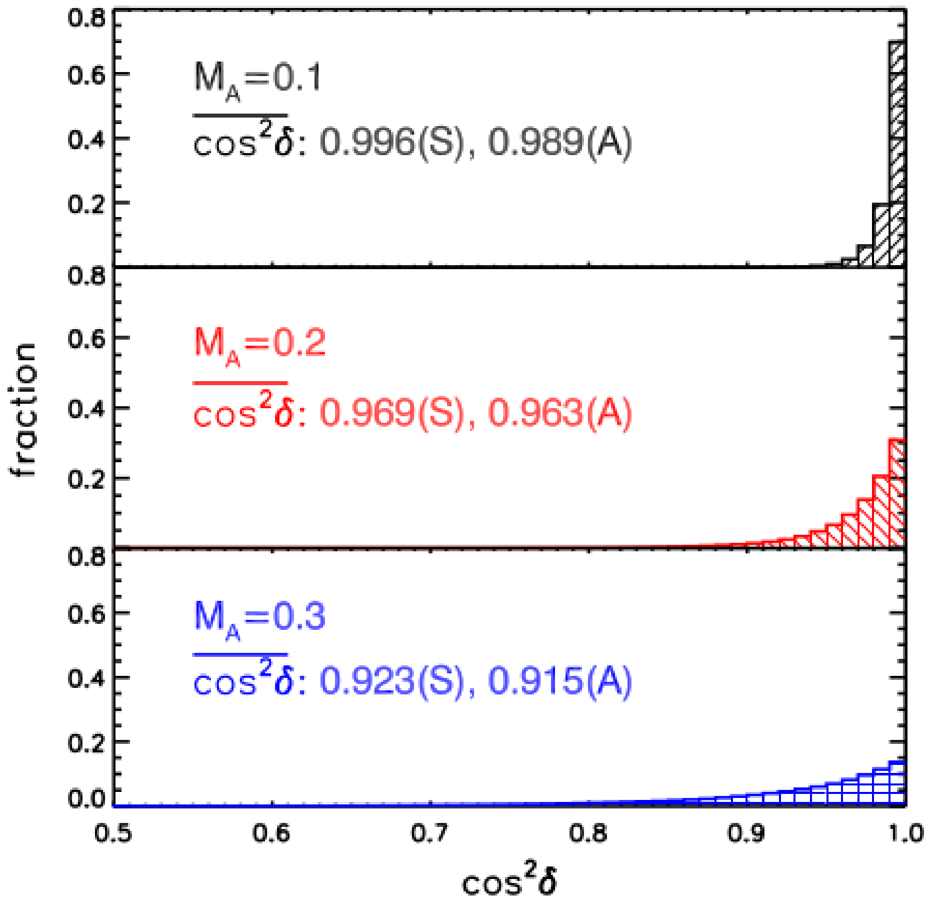

M_A=0.1
cos²δ: 0.996(S), 0.989(A)
M_A=0.2
cos²δ: 0.969(S), 0.963(A)
M_A=0.3
cos²δ: 0.923(S), 0.915(A)
fraction
cos²δ
0.0
0.2
0.4
0.6
0.8
0.5
0.6
0.7
0.8
0.9
1.0

Fermi-LAT observation on the TeV halo

D(100GeV)~2x10^{26}cm^2/s,
(Dt$_{gem}$)$^{1/2}$~30pc ~ 7°

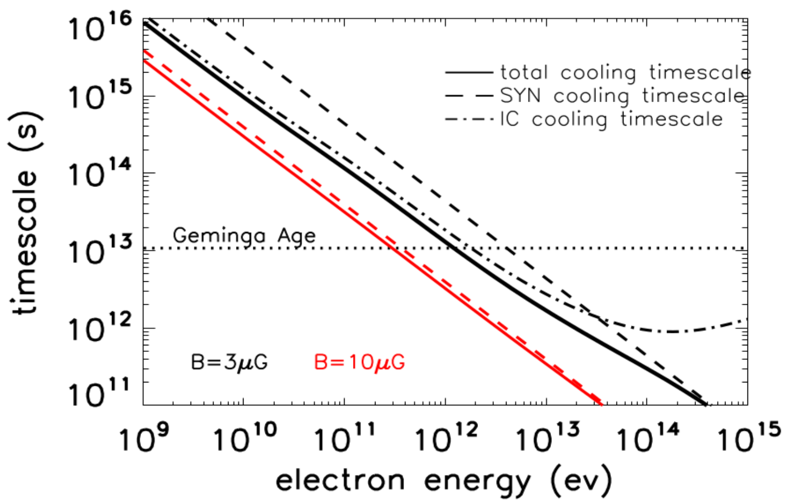

40°x40° ROI, 10-500GeV

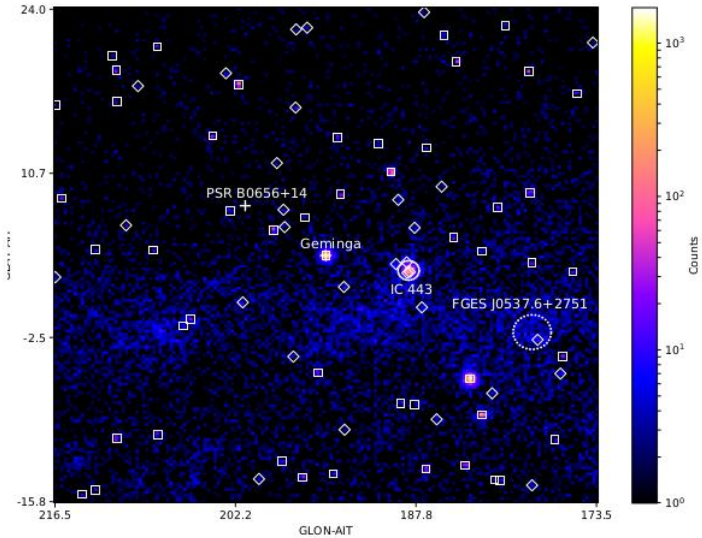

Count map

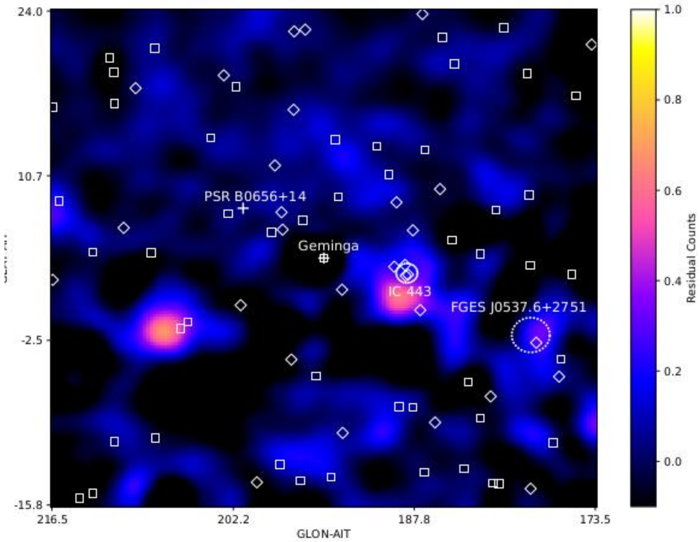

Residual map

Produce spatial templates (on the premise of fitting HAWC's observation

$$\frac{\partial N(E_e,r,t)}{\partial t} = \frac{1}{r^2}\frac{\partial}{\partial r}\left(r^2 D(E_e,r)\frac{\partial N}{\partial r}\right) - \frac{\partial}{\partial E_e}\left(\dot{E}_e N\right) + Q(E_e,t)\delta(r)$$

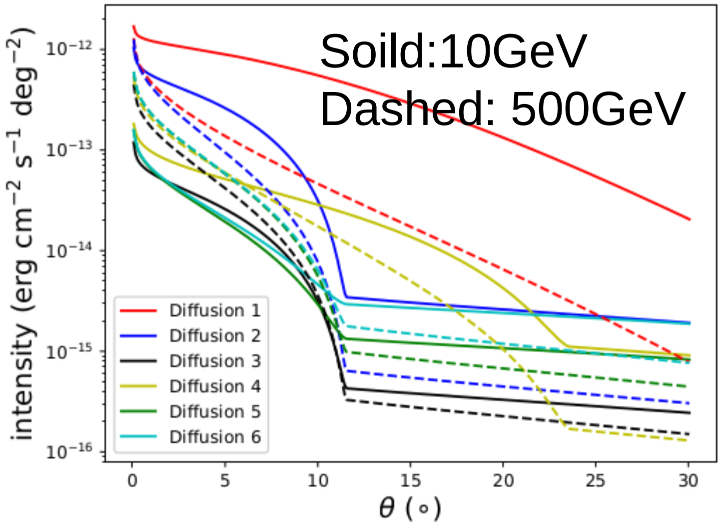

Line of sight integration

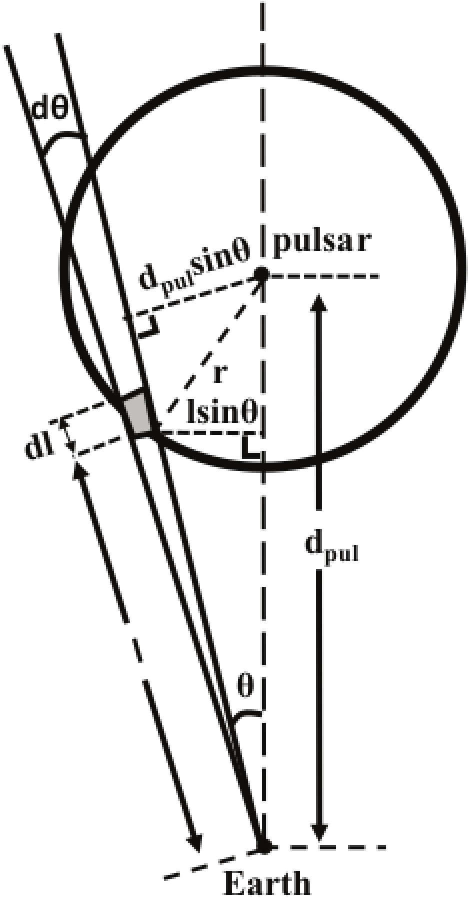

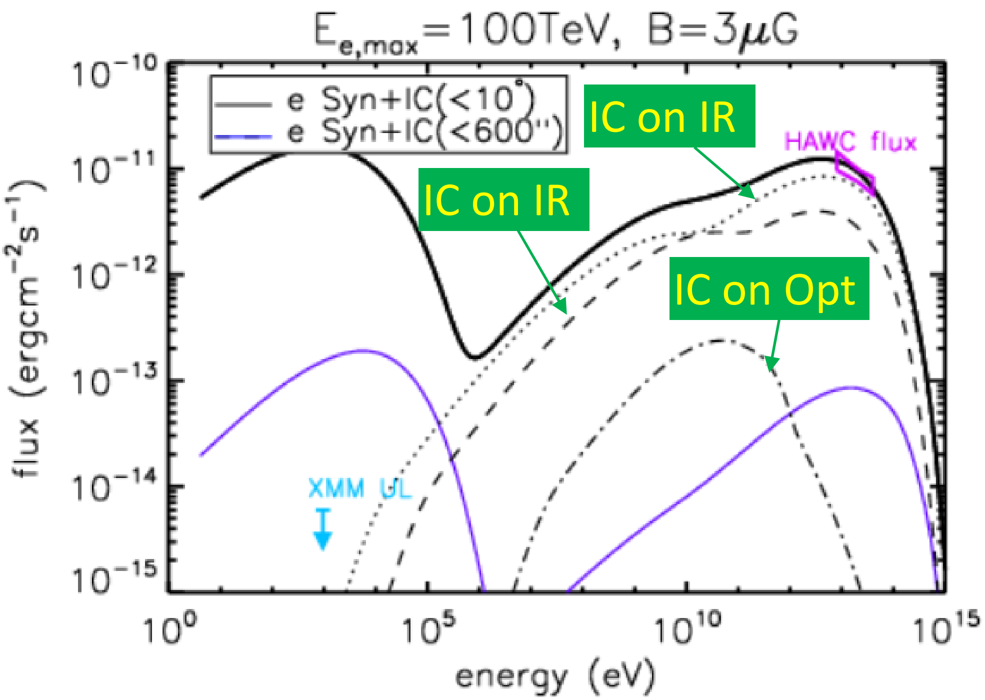

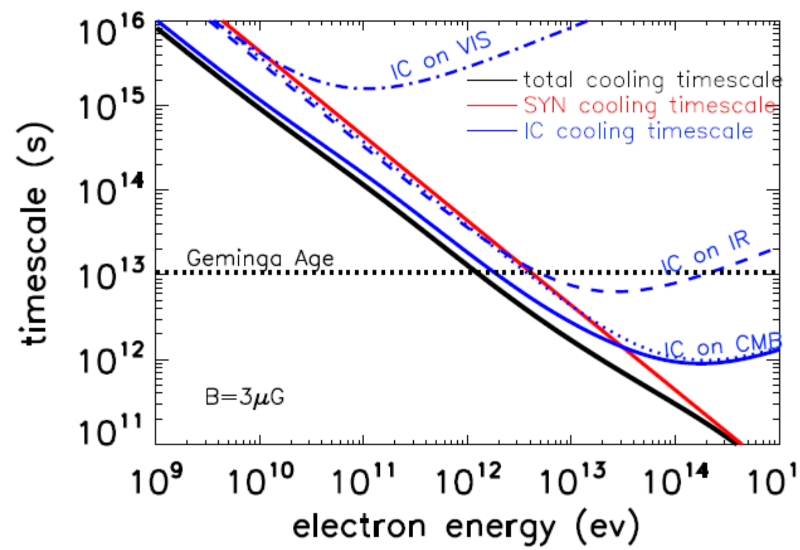

$$f_{IC} \propto N_e P_{IC} = C E_e^{2-s} t_{\mathrm{IC}}^{-1}$$

$$P_{IC} = \frac{E_e}{t_{IC}}$$

$$N_e \approx E_e \frac{dN_e}{d\gamma_e} = C E_e^{1-s}$$

$$\frac{f_{IR}}{f_{CMB}} = \left(\frac{E_{e,IR}}{E_{e,CMB}}\right)^{2-s} \frac{t_{IC,CMB}}{t_{IC,IR}}$$

$$E_\gamma \simeq \frac{(E_e/m_e c^2)^2 \epsilon}{1+\epsilon E_e/m_e^2 c^4}$$

Considering KN effect (recoil)

$$E_{e,IR}(20TeV) = 50TeV$$

$$E_{e,\mathrm{CMB}}(20TeV) = 100TeV$$

Distribution of 100GeV positron density in anisotropic diffusion scenario, assuming the global mean B field between Geminga and Earth is aligned with LOS (most optimistic case)

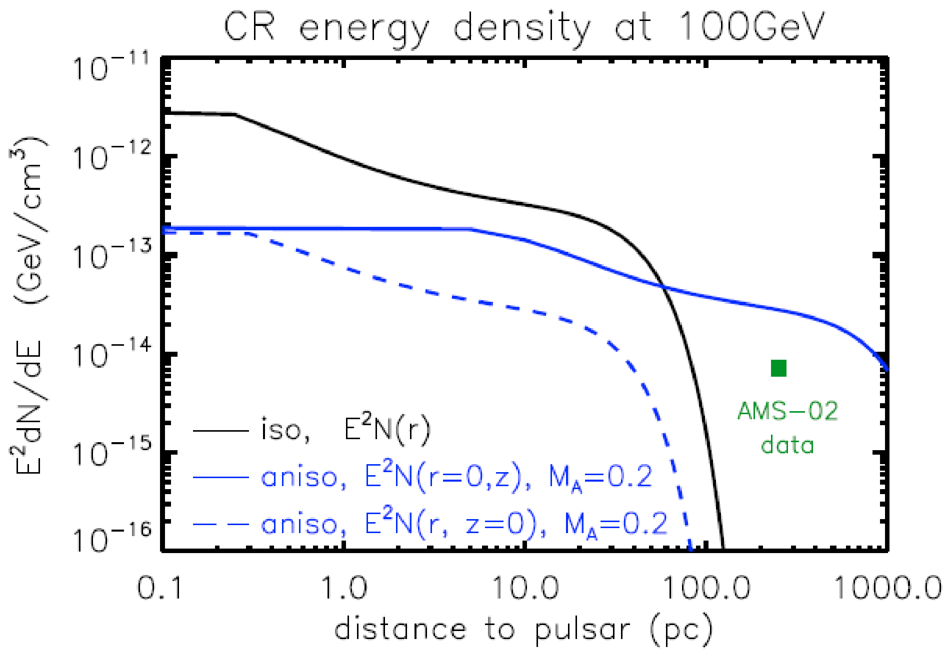

NANJING UNIVERSITY

HAWC's best-fit parameters

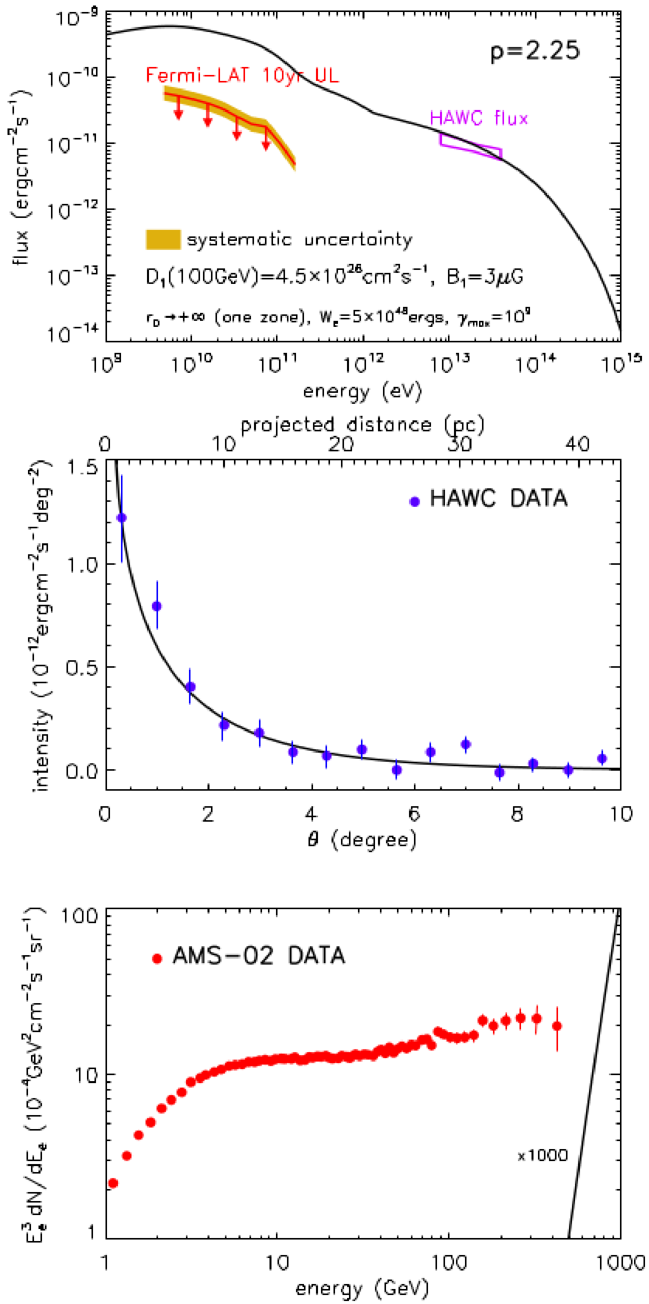

Two diffusion zone

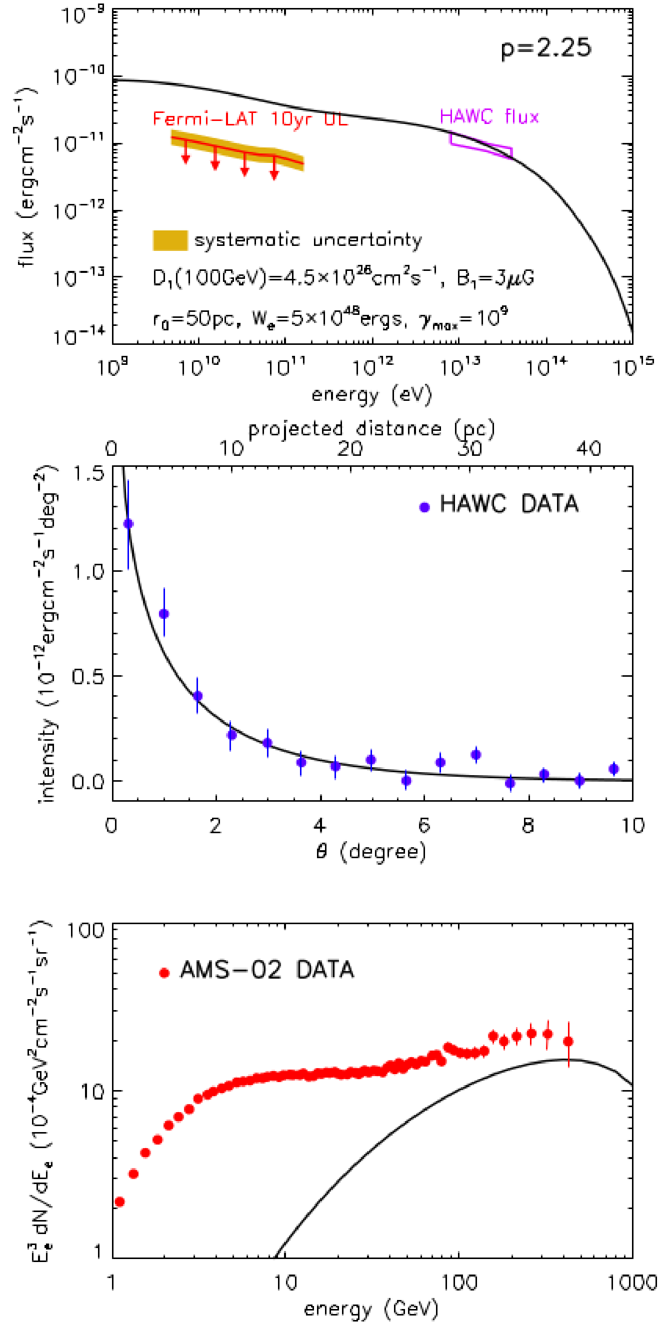

A harder injection spectrum

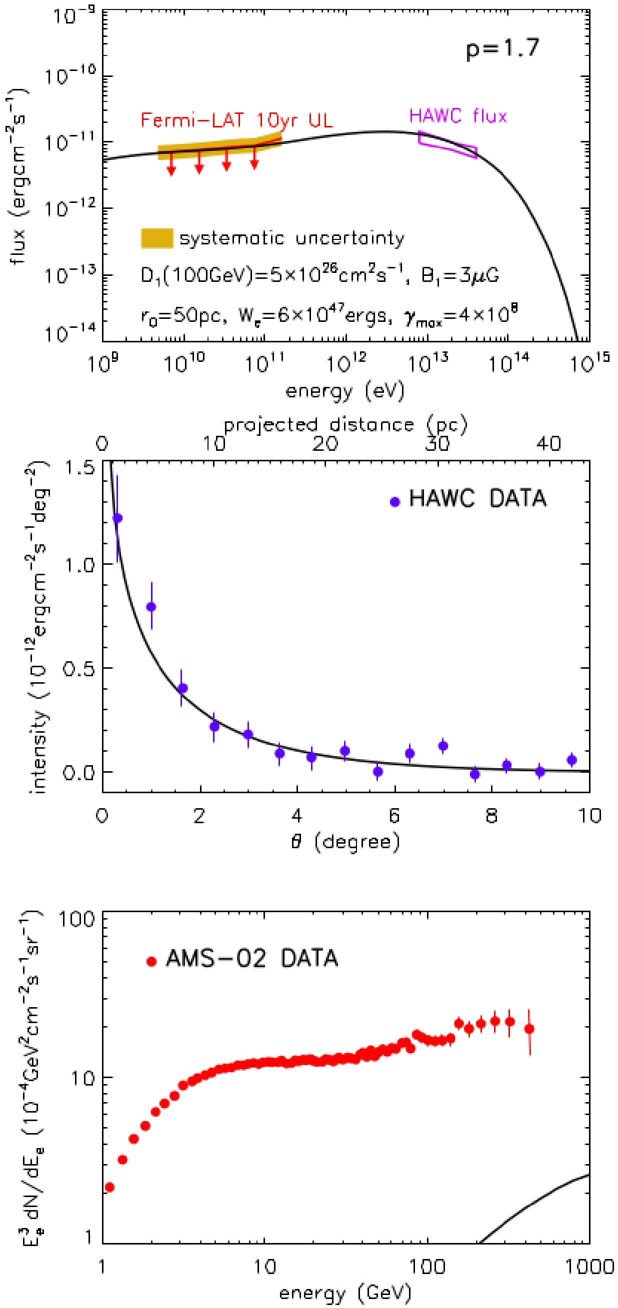

Energy-independent diffusion

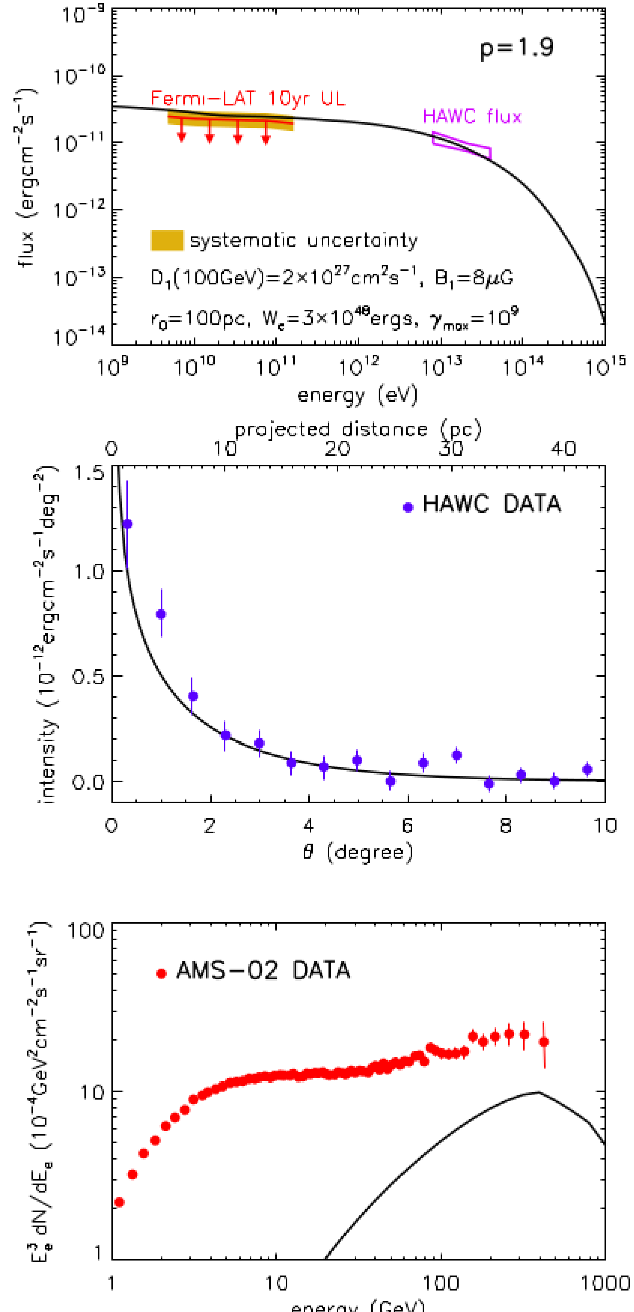

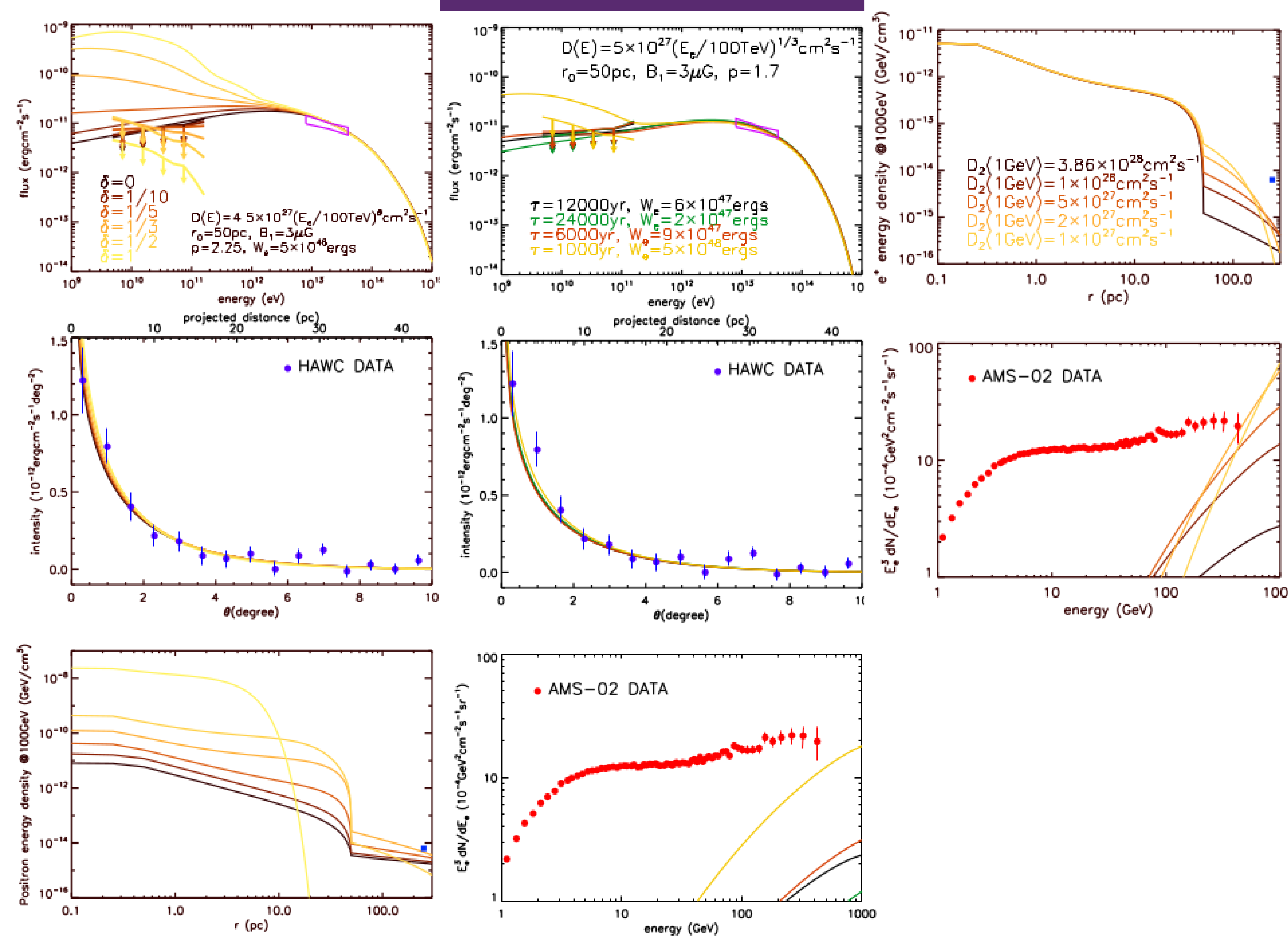

D(E)=4.5×10^27(E_e/100TeV)^δ cm^2s^-1
r_0=50pc, B_1=3μG
p=2.25, W_e=5×10^48ergs
δ=0
δ=1/10
δ=1/5
δ=1/3
δ=1/2
δ=1
flux (ergcm^-2s^-1)
energy (eV)
D(E)=5×10^27(E_e/100TeV)^1/3 cm^2s^-1
r_0=50pc, B_1=3μG, p=1.7
τ=12000yr, W_e=6×10^47ergs
τ=24000yr, W_e=2×10^47ergs
τ=6000yr, W_e=9×10^47ergs
τ=1000yr, W_e=5×10^48ergs
D_2(1GeV)=3.86×10^28cm^2s^-1
D_2(1GeV)=1×10^28cm^2s^-1
D_2(1GeV)=5×10^27cm^2s^-1
D_2(1GeV)=2×10^27cm^2s^-1
D_2(1GeV)=1×10^27cm^2s^-1
e^+ energy density @100GeV (GeV/cm^3)
r (pc)
projected distance (pc)
HAWC DATA
intensity (10^-12ergcm^-2s^-1deg^-2)
θ(degree)
AMS-02 DATA
E_e^3 dN/dE_e (10^-4GeV^2cm^-2s^-1sr^-1)
energy (GeV)
Positron energy density @100GeV (GeV/cm^3)

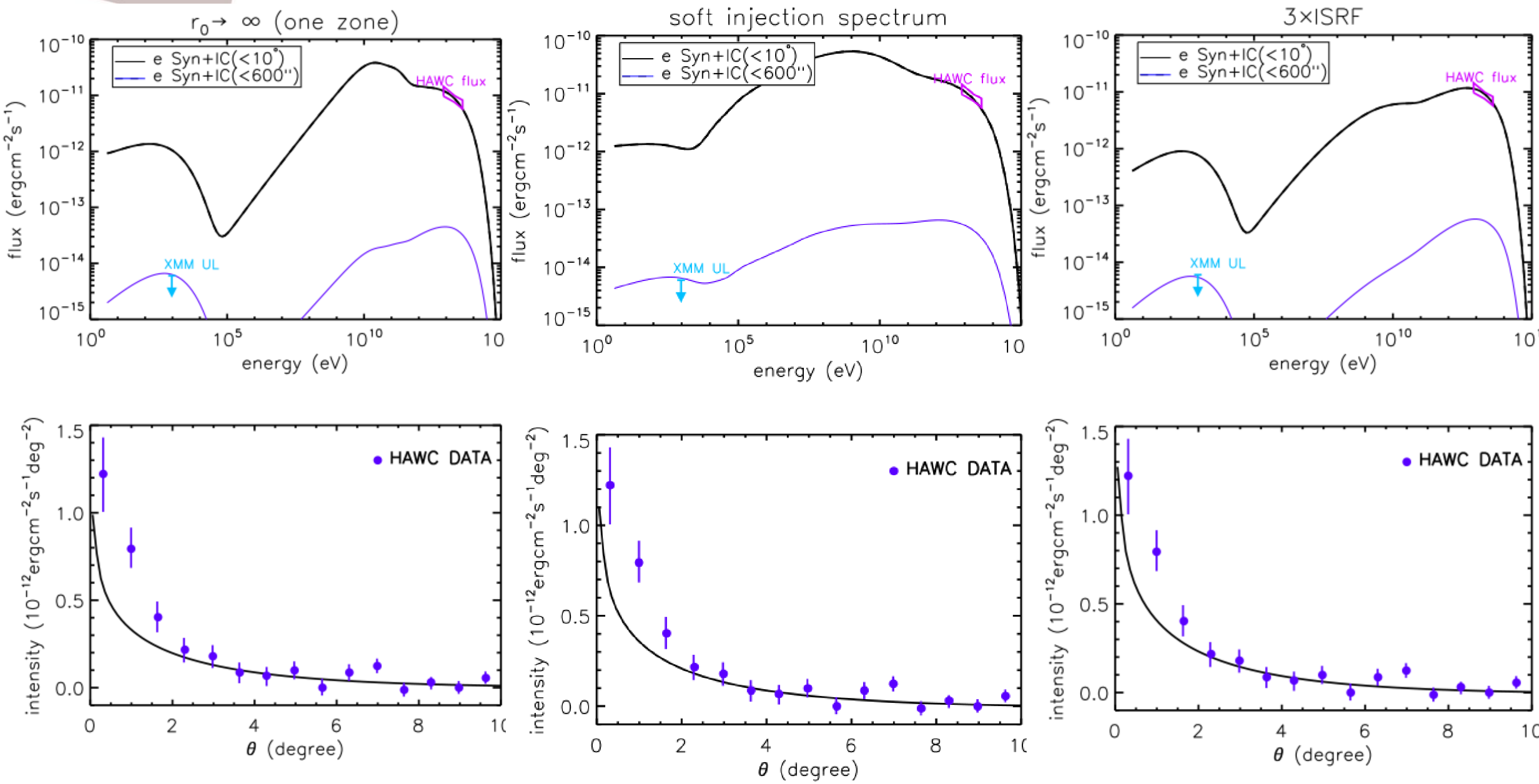
$r_0 \to \infty$ (one zone)
soft injection spectrum
3×ISRF
e Syn+IC(<10°)
e Syn+IC(<600'')
HAWC flux
XMM UL
flux (ergcm^{-2}s^{-1})
energy (eV)
HAWC DATA
intensity (10^{-12}ergcm^{-2}s^{-1}deg^{-2})
θ (degree)

B=0.9μG